

Fluidized Bed Steam Reforming (FBSR) Mineralization for High Organic and Nitrate Waste Streams for the Global Nuclear Energy Partnership (GNEP) - 8314

C.M. Jantzen and M.R. Williams
Savannah River National Laboratory
Aiken, SC 29808, USA

ABSTRACT

Waste streams that may be generated by the Global Nuclear Energy Partnership (GNEP) Advanced Energy Initiative may contain significant quantities of organics (0-53 wt%) and/or nitrates (0-56 wt%).[‡] Decomposition of high nitrate streams requires reducing conditions, e.g. organic additives such as sugar or coal, to reduce the NO_x in the off-gas to N₂ to meet the Clean Air Act (CAA) standards during processing. Thus, organics will be present during waste form stabilization regardless of which GNEP processes are chosen, e.g. organics in the feed or organics for nitrate destruction. High organic containing wastes cannot be stabilized with the existing HLW Best Developed Available Technology (BDAT) which is HLW vitrification (HLVIT) unless the organics are removed by preprocessing. Alternative waste stabilization processes such as Fluidized Bed Steam Reforming (FBSR) operate at moderate temperatures (650-750°C) compared to vitrification (1150-1300°C). FBSR converts organics to CAA compliant gases, creates no secondary liquid waste streams, and creates a stable mineral waste form that is as durable as glass. For application to the high Cs-137 and Sr-90 containing GNEP waste streams a single phase mineralized Cs-mica phase was made by co-reacting illite clay and GNEP simulated waste. The Cs-mica accommodates up to 30% wt% Cs₂O and all the GNEP waste species, Ba, Sr, Rb including the Cs-137 transmutation to Ba-137. For reference, the cesium mineral pollucite (CsAlSi₂O₆), currently being studied for GNEP applications, can only be fabricated at ≥1000°C. Pollucite mineralization creates secondary aqueous waste streams and NO_x. Pollucite is not tolerant of high concentrations of Ba, Sr or Rb and forces the divalent species into different mineral host phases. The pollucite can accommodate up to 33% wt% Cs₂O.

INTRODUCTION

As part of the United States Advanced Energy Initiative, the Department of Energy (DOE) has launched the GNEP Technology Demonstration Program (TDP). The GNEP-TDP will demonstrate technologies needed to implement a closed fuel cycle that enables recycling and consumption of spent nuclear fuel in a proliferation-resistant manner. Several different flowsheets are being considered for the separation of the principal heat-generating isotopes Cs-137 and Sr-90 from the wastes generated from energy production. These isotopes will be separated and stabilized into a single waste form along with Rb and Ba* and stored at a special facility where the isotopes will be allowed to decay for approximately 10 half lives.[§] This strategy would relieve the federal geologic repository of the anticipated short-term (300 year) heat load. The repository volume will be used less efficiently if heat-producing waste forms (such as those containing Cs-137 and Sr-90) are geologically disposed. Therefore, removing Cs-137 and Sr-90 during the reprocessing stage is needed if repository space is to be conserved.

[‡] on a dry weight percent basis at 60°C

* the Cs and Sr are stripped from the waste stream but the stripping agents carry along Ba and Rb in the waste stream as well. For brevity, the stream is referred to as Cs/Sr only.

[§] The half life of ¹³⁷Cs is 30.2 years, and the half life of ⁹⁰Sr is 29.1 years.

Research is necessary to develop an acceptable waste form for the Cs/Sr removed. This waste form must be economically feasible and meet yet-to-be-developed technical requirements for the storage facility. If, after 300 years of storage, the waste can be classified as low-level waste (LLW), both the waste form and the disposal options become simpler. There are several challenges inherent in the Cs/Sr baseline disposal scenario which includes the ability to show that 100 years or more of institutional control is possible, that >100 years storage constitutes disposal, and that the Cs/Sr stream is not high-level waste (HLW). Alternative disposal scenarios are:

- Processing of the Cs/Sr waste after 300 years of storage to a form that is not hazardous, i.e., can pass the Toxicity Characteristic Leach Procedure (TCLP), followed by disposal at either a LLW or HLW site.
- Processing the Cs/Sr waste stream as generated to a waste form that can be disposed of at the federal geologic repository for HLW.

Mineral waste forms are more suitable for the high heat load Cs/Sr baseline waste streams. A single phase mineral waste form that could accommodate the Cs, Sr, Ba, and Rb is easier to qualify than a multiphase mineral assemblage where Cs and Rb would likely be in one phase and Ba and Sr. In multiphase mineral waste forms one must determine the partitioning of the species amongst the phases in order to qualify the waste form. Since ~53% of the Cs-137 decays to Ba-137 and ~48% of the Sr-90 decays to Zr-90, the Cs-137 host phase must also be able to accommodate the decay to Ba-137 and the Sr-90 host phase must also be able to accommodate the decay to Y-90 and ultimately Zr-90. The Ba-137 and Zr-90 decay products must be accommodated by the mineral structure so that the phase(s) do not alter in a deleterious manner, e.g. volume expansion or contraction. This can only be simulated by demonstrating that phase pure balanced crystal-chemical substitutions of the Cs/Sr and the Ba/Zr decay products are *possible*, e.g. determine the maximum solubility of Ba in single phase $\text{CsAlSi}_2\text{O}_6$ (pollucite) or some other mineral host and/or by subjecting single phase $\text{CsAlSi}_2\text{O}_6$ to accelerated radiation treatment to induce the Cs-137 to Ba-137 transformation.

The scope of this study was to examine a variety of clays that would react with the simulated Cs/Sr GNEP streams to form an acceptable single mineral host phase or a multiphase mineral phase assemblage. Due to the high nitrate and organic content of the Cs/Sr GNEP streams, and the volatility of Cs-137 when processing, the advanced FBSR technology which limits process temperatures to 650-750°C and is CAA compliant was examined extensively.

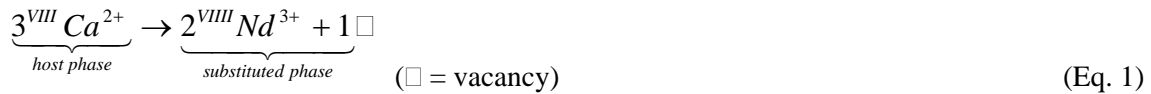
THEORY: ELECTRICALLY BALANCED CRYSTAL-CHEMICAL SUBSTITUTIONS

Crystal-chemical substitutions must be electrically balanced. [1,2] When a monovalent cation decays to a divalent cation, the substitutions must be coupled to retain the electrical balance of the host phase without destroying the integrity of the phase: the lattice site must be of suitable size and bond coordination to accept the transmutation. While the bonding in glass is considered random and thus, flexible enough to accommodate a wide variety of transmutations involving changes in valence and atomic size, the bonding in crystalline ceramic or mineral phases can only maintain charge balance in one of two ways: (1) if sufficient lattice vacancies exist or (2) if a variable valence cation like Fe or Ti is present in a neighboring lattice site for charge balance. Both scenarios assume that the variable valence cations do not change lattice sites and that the charge balancing cations are in the same host phase in nearby lattice sites. The lattice site must be

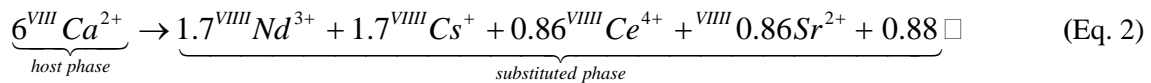
of sufficient size or flexible enough to accommodate the decaying cation. It is advantageous if the lattice site has irregular coordination or is distorted as will be shown in the examples below.

Lattice Vacancy Substitutions: Examples

The solubility or tolerance of a ceramic or mineral phase as a host for a substituted cation of a different valence can be studied by performing coupled substitutions on the phase pure mineral host phase. For example, coupled substitutions[§] of the type



have been successful [1,2] in the oxyapatite ($Ca_6[SiO_4]_3$) structure forming completely substituted $Nd_4\Box_2[SiO_4]_3$ where 2/3 of the lattice sites have Nd^{3+} and 1/3 are vacant. In the oxyapatite structure the Ca^{2+} is normally in VIII-fold coordination and has a 1.12 Å [3,4] atomic radius. The Nd^{3+} cation in VIII-fold coordination also has an atomic radius of 1.12 Å [3,4]. Felsche showed that the rare earth elements La^{3+} through Lu^{3+} can substitute for Ca^{2+} and form oxyapatites, $RE_{4.67}\Box_{0.33}[SiO_4]_3O$. [5] McCarthy and Davidson [6], showed that even more complex, but coupled, substitutions were possible in the oxyapatite structure such as

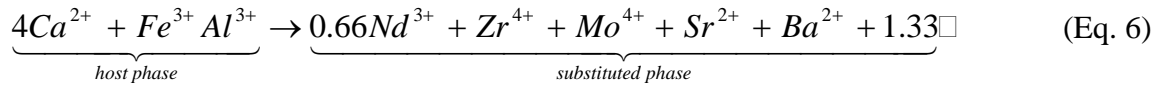
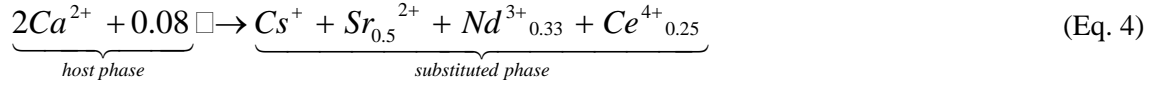


where the atomic radius, r , of Cs^{+} in VIII-fold coordination is 1.82 Å, Ce^{4+} in VIII-fold coordination is 0.97 Å, and Sr^{2+} in VIII-fold coordination is 1.25 Å. In this case small radii cations such as Ce^{4+} are mixed with large radii cations like Cs^{+} so that individual lattice sites can distort without perturbing the entire crystal structure. Note that the exchanging cations are always in the same lattice site of the same host phase [1,2,5,6].

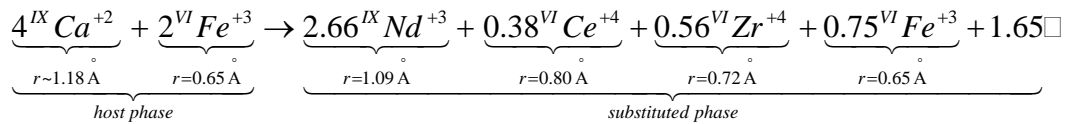
The substitutions shown in Eq. 1 and Eq. 2 were also demonstrated [1,2] to be possible in many other Ca-bearing minerals such as larnite (Ca_2SiO_4 or β - C_2S), alite (calcium trisilicate or Ca_3SiO_5 or C_3S), C_3A ($Ca_3Al_2O_6$), and C_4AF ($Ca_4Al_2Fe_2O_{10}$). In larnite half the Ca^{2+} is in VI-fold coordinated sites and half in VIII-fold coordinated sites. The coordination sites in C_2S are highly irregular in shape [7] which makes the Ca^{2+} sites ideal lattice sites for substitutions of a variety of mono- and tri-valent cations of similar size. Likewise, the Ca^{2+} cation in alite is in irregular VI-fold coordination: the oxygens are concentrated to one side of each Ca^{2+} cation, leaving a “hole” on the other side that is large enough to accommodate another Ca^{2+} [7] or possibly a substituted cation. The C_3S structure, therefore, has ample vacancies for charge substituting cations. In the C_3A structure there are also two types of Ca^{2+} cations: half of the Ca^{2+} cations are at the corners of the lattice cell in regular VI-fold coordination while the inner cell half have irregular IX-fold coordination.[7] The Al^{3+} in the C_3A structure are irregularly coordinated in mixed VI and IV fold coordination, e.g. AlO_4 and AlO_6 groups.[7] In calcium aluminoferrite (C_4AF) the Ca^{2+} is also in irregular IX-fold coordination and both FeO_4 and FeO_6 (Fe^{3+} in IV and VI coordination)

[§] Notation such as ^{VIII}Ca will be used to designate the coordination of the lattice sites, in this case octahedral VIII-fold coordination for the Ca^{2+} lattice site

exist.[7] This allowed Jantzen, et. al. [8,9] to make substitutions for Ca^{2+} (Eq. 1) in each phase (up to ~ 15 mole%) and the following additional substitutions:

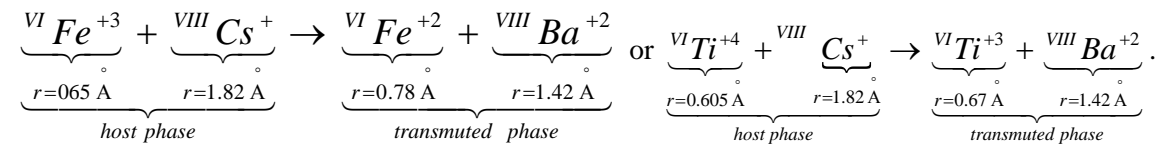


In addition, La^{3+} , Lu^{3+} , Yb^{3+} , and Ce^{3+} were also successfully substituted for Ca^{2+} in $\beta\text{-C}_2\text{S}$ and the oxyapatite structures.[1,2] In C_4AF or $4\text{CaO}\cdot\text{Al}_2\text{O}_3\cdot\text{Fe}_2\text{O}_3$ where the Fe^{3+} is in IV-fold and VI-fold coordination, Zr^{4+} and Ce^{4+} were successfully substituted for octahedral Fe^{3+} when the cation Nd^{3+} was substituted for Ca^{2+} as follows:



Charge Balance Substitutions:Examples

A transition metal cation with variable valance has also been suggested to maintain charge neutrality during decay of $\text{Cs}^+ \rightarrow \text{Ba}^{2+}$ or $\text{Sr}^{2+} \rightarrow \text{Y}^{3+} \rightarrow \text{Zr}^{4+}$, for example:



These types of crystal-chemical substitutions have been studied in (1) SYNROC (SYNthetic ROCK) titanate phases such as zirconolite ($\text{CaZrTi}_2\text{O}_7$), perovskite (CaTiO_3), and hollandites (nominally $\text{Ba}(\text{Al},\text{Ti})_2\text{Ti}_6\text{O}_{16}$) [10] and (2) in high alumina tailored ceramic phases such as magnetoplumbites [11,12]. The magnetoplumbites (discussed below) are also found as a minor component in SYNROC when the waste being stabilized is high in Al.[13]

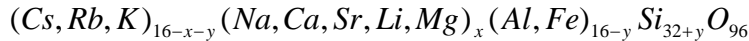
In the SYNROC phase assemblages, the hollandite phase is the Cs^+ host phase. The structure can be written as $\text{Ba}_x\text{Cs}_y(\text{Al},\text{Fe})_{2x+y}\text{Ti}_{8-2x-y}\text{O}_{16}$ where $x+y$ must be <2 . [14] There are two types of octahedral sites. One accommodates trivalent cations like Al^{3+} , Ti^{3+} , and Fe^{3+} while the other accommodates Ti^{4+} . The Cs^+ is accommodated in tunnels that normally accommodate the Ba^{2+} cation. The Cs-Ba lattice sites are VIII-fold coordinated [10, 14]. The substitution is ordered upon fabrication and incommensurate superstructures result when Cs^+ substitutes for Ba^{2+} . [13] Cesium has been experimentally substituted for Ba when Fe^{3+} is substituted for Ti^{3+} in the VI-fold sites and $\underbrace{\overset{\text{VIII}}{\text{Cs}^{+0.28}}}_{\text{A site}} \underbrace{\overset{\text{VIII}}{\text{Ba}^{2+1.00}}}_{\text{B site}} \underbrace{\overset{\text{VI}}{\text{Al}^{3+1.46}} \overset{\text{VI}}{\text{Fe}^{3+0.82}}}_{\text{C site}} \overset{\text{VI}}{\text{Ti}}_{5.72}\text{O}_{16}$ has been fabricated by sintering in

air at 1320°C.[14] A Ba-Al hollandite ($\text{Ba}_{1.16}\text{Al}_{2.32}\text{Ti}_{5.68}\text{O}_{16}$) was both electron irradiated (1-2.5MeV) and β -irradiated (4×10^8 to 7×10^9 Gy) and found to contain Ti^{3+} centers and O_2^- superoxide ions which confirmed the mechanism of charge balance during decay.[14] Theoretically, the limiting y value in hollandite is 0.81 Cs which corresponds to a 9.54 wt% waste loading of Cs_2O .[15]

In the tailored ceramics magnetoplumbites $\text{X}(\text{Al,Fe})_{12}\text{O}_{19}$ are the Cs and Ba host where Sr, Ba, $\text{Cs}_{0.5} + \text{La}_{0.5}$ or $\text{Na}_{0.5}\text{RE}_{0.5}$ occupy the X site which is XII-fold coordinated and both $\text{Cs}^+/\text{Ba}^{2+}$ - $\text{Fe}^{3+}/\text{Fe}^{2+}$ or $\text{Cs}^+/\text{Ba}^{2+}$ - $\text{Ti}^{4+}/\text{Ti}^{3+}$ type decays can occur. The magneto-plumbites are accommodating structures because they have spinel blocks with both IV-fold and VI-fold coordinated sites for multivalent cations and interspinel layers which have unusual V-fold sites for small cations. The interspinel layers also accommodate large cations of 1.15-1.84 Å, replacing oxygen in XII-fold sites in the anion close packed structure.[16] The large ions may be monovalent, divalent, or trivalent with balancing charge substitutions either in the interspinel layer ($\text{Na}_{0.5} + \text{La}_{0.5}$) or between the interspinel layer and the spinel blocks ($\text{Cs}^+/\text{Ba}^{2+}$ - $\text{Fe}^{3+}/\text{Fe}^{2+}$ or $\text{Cs}^+/\text{Ba}^{2+}$ - $\text{Ti}^{4+}/\text{Ti}^{3+}$).[11]

Charge Balance Substitutions Proposed for GNEP Cs-Mineral Host

Pollucite ($\text{CsAlSi}_2\text{O}_6$) is the mineral currently being investigated for Cs-137 sequestration from the GNEP waste streams. It is fabricated by mixing GNEP Cs/Sr wastes with montmorillonite clay, cold isostatic pressing into discs, and sintering in air at 1000°C.[17] If pollucite is to be used as the Cs-137 host phase for the Cs/Sr GNEP streams it must be able to accommodate Cs, Ba, and multivalent cations such as Fe^{3+} and Fe^{2+} or Ti^{3+} and Ti^{4+} in the same phase. It can easily be seen that the mineral pollucite becomes electrically unbalanced if it does not accommodate Fe^{3+} in its lattice as an electron donor to form Fe^{2+} when the monovalent Cs^+ decays to divalent Ba^{+2} . While defect pollucites like



are known in nature, and can accommodate Rb and Sr in their structure, they have limited solubility for divalent and trivalent species other than Al^{3+} , e.g. the maximum Ca^{2+} content reported is 0.77 wt%, the maximum Mg^{2+} content is 0.39 wt%, and the maximum Fe^{3+} content is reported to be ~0.43 wt%.[18] However, iron-pollucites ($\text{CsFeSi}_2\text{O}_6$) have been made hydrothermally as well as compositions intermediate between $\text{CsAlSi}_2\text{O}_6$ - $\text{CsFeSi}_2\text{O}_6$.

In pollucite the Cs atoms are XII coordinated [18] and occupy the sites that the water molecules normally occupy in hydrated pollucite. In anhydrous pollucite the sites normally occupied by water molecules are vacant. Cs^+ in XII coordination has an atomic radius of 1.88 Å while Ba^{2+} has an atomic radius of 1.60 Å [18]. Preferably, the Ba-137 should be accommodated in the same lattice site as the Cs-137 and the Fe^{+2} should be accommodated in the same lattice site as the Fe^{+3} since the atoms will not exchange lattice sites or host phases.

The tolerance of phase pure pollucite for Ba^{2+} and $\text{Fe}^{2+}/\text{Fe}^{3+}$ needs to be studied to determine if the $\underbrace{\text{IV Fe}^{+3}}_{r=0.49 \text{ \AA}} + \underbrace{\text{XII Cs}^+}_{r=1.88 \text{ \AA}} + \square \rightarrow \underbrace{\text{IV Fe}^{+2}}_{r=0.63 \text{ \AA}} + \underbrace{\text{XII Ba}^{+2}}_{r=1.60 \text{ \AA}} + \square$ decay can indeed occur without volume

expansion or contraction of the lattice since it is unlikely that Fe^{2+} will be stable in tetrahedral coordination. In addition, a phase pure pollucite needs to undergo accelerated radiation testing as performed on hollandite. [14] These effects cannot be simulated by mixing Cs and Ba into the

starting materials and attempting to make a defect pollucite as a mixture of pollucite $\text{CsAlSi}_2\text{O}_6$ and celsian $[\text{Ba}(\text{Al}_2\text{Si}_2\text{O}_8)]$ results as shown later in this paper.

FBSR PROCESSING: CLEAN AIR ACT (CAA) COMPLIANCE

Mineralization during FBSR processing takes place at moderate temperatures, i.e. 650-750°C. These moderate temperatures do not volatilize radionuclides like Cs-137. In FBSR the organic compounds are pyrolyzed to CO_2 via the water gas shift reaction (WGSR) while nitrate/nitrite species are converted to N_2 through reactions with superheated steam, which is the fluidizing media.[19,20,21] The FBSR technology[§] has been determined to be CAA compliant by Region IV Environmental Protection Agency (EPA). In addition, the FBSR process is Hazardous Waste Combustor (HWC) Maximum Achievable Control Technology (MACT) compliant.[22,23]

FBSR PROCESSING: NANOSCALE MINERALIZATION

The FBSR mineralized waste forms are normally produced by co-processing kaolin clay with sodium bearing wastes. The multiphase mineral assemblages produced are Na-Al-Si feldspathoid minerals with cage and ring structures that bond radionuclides such as Tc-99 and Cs-137 and anions such as SO_4 , I, F, and Cl. Mineralization occurs at the moderate FBSR temperatures because the temperature is in the range in which most clays become amorphous at the nanoscale, e.g. kaolin, bentonite, montmorillonite, and illite. The clays lose their waters of hydration at the FBSR temperatures which destabilizes the Al^{3+} cation in their structure. The alkali in the waste, “alkali activates” the unstable Al^{3+} cation to form new mineral phases and the fluidizing agent, steam, catalyzes the mineralization. In the absence of steam many of these mineral phases only form at temperatures of 1200-1500°C.

FBSR PRODUCT: DURABILITY AND MONOLITH FORMATION

The FBSR mineral waste form is granular in nature. As a granular product it has been shown to be as durable as Hanford’s LAW glass during testing with ASTM C-1285-02 known as the Product Consistency Test (PCT) [24,25,26,27,28] and testing with the Single Pass Flow Through Test (SPFT) [27,29,30,31]. Hanford Envelope A and Envelope C simulants both performed well during PCT and SPFT testing and during subsequent performance assessment modeling.[29,32] This is partially due to the high aluminosilicate content of the mineral product which provides a natural aluminosilicate buffering mechanism [25,26,27] that inhibits leaching and is known to occur in nature during weathering of aluminosilicate mineral analogs [33].

While the durability testing of the FBSR granular product indicates that the granular product is as durable as vitreous waste forms, monolithing of the granular product may be needed for control of respirable fines and/or for the intruder scenario for shallow land burial. Therefore, monolithing of the FBSR product was investigated in ordinary Portland cement (OPC), Ceramicrete, and hydroceramics.[34,35] Additional monolithing agents are under study.

EXPERIMENTAL

Simulants of the three GNEP waste streams were prepared and analyzed. Two were high organic and one was high nitrate. One of the high organic simulants known as the Engineering Alternative Study (EAS) stream and the high nitrate stream known as the Fission Product EXtraction (FPEX) stream were tested with a variety of clays and zeolite precursors. The clays

[§] The Studsvik, Inc. facility in Erwin, TN pyrolyzes organic Cs-137 and Co-60 resins up to 400R/hr.

included pure montmorillonites, bentonites (mixtures of montmorillonite and beidellite), kaolins, hectorites (Li montmorillonites), and illites (Table I). The zeolites included Linde IE-95 (a mixture of chabazite and erionite) used to extract Cs from aqueous streams and clinoptilite (Table I). The illites and zeolites were chosen because of their known preference for sorbing Cs from aqueous wastes. [36]

The simulants were evaporated due to the low wt% solids content. Evaporation was stopped before supersaturation caused any crystalline phases to precipitate. The Mincalc-Rev.3 strategy developed at SRNL and used for pilot scale FBSR demonstrations since 2004 was employed to calculate the ratios of evaporated simulant to clay to form the desired phases. Two different strategies were used:

- substitution of Cs,Rb,Ba and Sr oxides (100 wt%) into one phase such as pollucite or Cs-mica
- substitution of Cs and Rb oxides (46-52 wt%) only into pollucite or Cs-mica allowing Ba/Sr oxides (48-54 wt%) to form a secondary phase such as the Ba feldspar known as celsian.

SRNL developed a laboratory scale method in 2003 to sequentially simulate the reactions that occur simultaneously during FBSR processing. The first step includes the nitrate/organic destruction, the water gas shift reactions (WGSR), and the REDuction/OXidation (REDOX) reactions. The first reaction step is performed at the nominal FBSR operation temperatures (650-725°C). The second step induces the hydrothermal synthesis of the zeolite mineral precursor phases in Parr bombs (i.e., Parr pressure vessels made of 316 stainless steel) at 90°C and the third step completes the dehydration reactions at the nominal FBSR temperatures (650-725°C). The laboratory scale methods (1 step and 3 step) have been demonstrated on Savannah River Site (SRS) wastes [37] to duplicate these reactions sequentially rather than simultaneously and produce the same mineral phases. This results from these laboratory scale tests for FBSR carbonate and silicate based phases were verified against pilot scale testing performed at INEEL.[38] The laboratory scale testing also showed that reactions with simulated FBSR bed materials could be duplicated and the use of an Fe^{+3} tracer in the waste form product could be used to monitor the f_{O_2} , f_{CO_2} , and f_{H_2} inside the crucibles. For example, crucible studies performed at SRNL had an $\text{Fe}^{2+}/\Sigma\text{Fe}$ ratio that indicated that the $-\log f_{\text{O}_2}$ values in the crucibles (static environment) were between -24 and -25 atmospheres. Pilot scale testing (dynamic environment) for the same feed at Hazen Research Inc. (HRI) corresponded to $-\log f_{\text{O}_2}$ values of -23 to -23.5 atmospheres which is within measurement error of the crucible studies.

The reductant of choice, when a reductant was used, was sucrose. A test matrix (Table II) was developed that varied two different levels of reductant (none and 2X stoichiometric) based on the following equations:

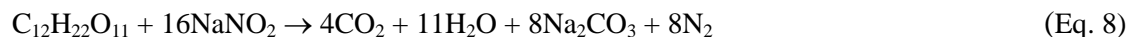
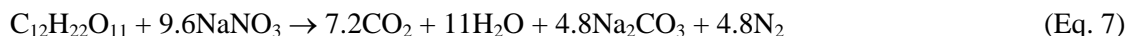


Table I. Clays and Zeolites Analyzed and Tested

Clay or Zeolite	Family	Vendor	Si:Al Atomic Ratio
Hectorite (Mg and Li instead of Al)	Montmorillonite	R. T. Vanderbilt Chemical Corp.	12.28
Window Peak Montmorillonite	Montmorillonite	Window Peak Trace Minerals	9.41
Clinoptilolite	Heulandite	Cycletrol Industries	4.58 (batch 1) 4.78 (batch 2)
Snow White Clinoptilolite	Heulandite	R. T. Vanderbilt Chemical Corp.	4.46
Chabazite/Erionite (IE-95)	Zeolite	Linde	3.61
Redart	Illite	Cedar Heights Clay	2.92
Keystone	Illite	KT Clay	2.87
Bentonite (mix of Montmorillonite and Bedillite)	Montmorillonite	Fisher	2.78
Sagger XX	Kaolin + qtz	KT Clay	1.89
Todd Light	Illite	KT Clay	1.78
Fireclay	Illite	Cedar Heights Clay	1.71
OptiKasT	Kaolin	KT Clay	1.04

The clay/simulant/reductant slurries were dried to peanut butter consistency. This ensures that some H₂O remains in the sample to create steam for the WGSR. Water is also available from the sugar reductant upon heating at the FBSR temperatures. Sealed crucible reaction was achieved by sealing high purity (99.999%) Al₂O₃ crucibles with nepheline (NaAlSiO₄) gel that softens and seals at a temperature lower than that at which the WGSR occurs. This causes the crucible to seal before the slurry reacts so that air inleakage does not occur during reaction. This is extremely important as air inleakage will alter the reactions as monitored by the measured REDOX ratio, Fe²⁺/ΣFe, and allow oxidizers and reductants to escape rather than reacting with the species in the slurry and additives. The Al₂O₃ crucibles also simulate Al₂O₃ bed material and determine if the FBSR product was adhering to the simulated bed media.

The sealed samples were placed in a calibrated furnace at the test temperature designated in the test matrix. This generated a combined atmosphere of steam, CO from decomposition of the sucrose, and CO₂ from carbonate species in the simulant thus duplicating the CO-steam environment necessary for the WGSR. The furnace was purged with 99.99% Ar to ensure that no O₂ mixed with any H₂ that diffused through the crucible seal thus eliminating any concern of explosive gas mixtures and duplicating the deoxygenated high CO₂ atmosphere of the FBSR process.

Product samples were analyzed by X-ray diffraction (XRD) to determine if the desired FBSR product was achieved. Samples were measured for Total Carbon (TC), Total Inorganic Carbon (TIC), and Total Organic Carbon (TOC). All samples were analyzed at SRNL for Fe²⁺/ΣFe ratio by the Baumann method [39]. The samples were dissolved using a LiBO₂ fusion and the solution analyzed by Inductively Coupled Plasma – Emission Spectroscopy (ICP-ES) for Al, Si, Na, Ti, Ba, Sr, Ti, Mn, and Zr to determine if the correct ratios of clay and simulant had been used during product formation. The solutions were also analyzed by ICP-Mass Spectroscopy

(ICP-MS) for Rb and Cs. Samples were dissolved by sodium peroxide fusion with a water uptake. These dissolutions were measured by Ion Chromatography (IC) for NO₂, NO₃, F, Cl and SO₄ to ensure that nitrate destruction was complete. Due to the large number of samples generated not all samples were analyzed for every analysis described above.

RESULTS

The GNEP laboratory tests results will be discussed in the following order:

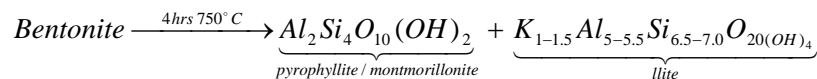
- scoping tests to determine the crucible residence time, e.g. 3, 6, 24, or 48 hours, and amount of reductant that best duplicated the FBSR REDOX while completely denitrating the feed and completely destroying the organics
- tests with clay and K₂NO₃ since the anhydrous K₂O-Al₂O₃-SiO₂ ternary system which forms leucite (KAlSi₂O₆) the analogue of pollucite (CsAlSi₂O₆) is known while the Cs₂O-Al₂O₃-SiO₂ and Rb₂O-Al₂O₃-SiO₂ ternary systems are not known.
- single step anhydrous tests with full GNEP simulant
- triple step (anhydrous-hydrous-anhydrous) GNEP tests with full simulant
- duplication of the GNEP bentonite press and sinter process (anhydrous pollucite formation at 1000°C) with full GNEP simulant

Scoping Tests: REDOX, Residence Time, Clay Type, and Clay Heat Treatment

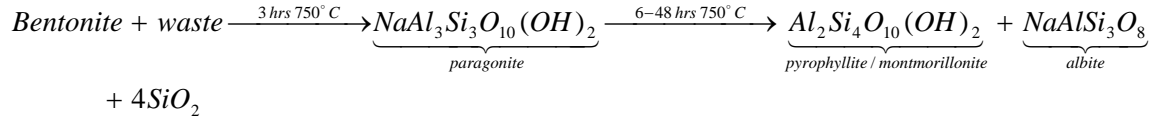
During the scoping tests Fisher bentonite, Sagger XX fine ball clay (kaolin rich), clinoptilite (Cycletrol and Snow White), IE-95 (chabazite and erionite in an Fe₂O₃ rich binder), and a variety of illites with different Si:Al atomic ratios (Redart, Todd Light, Fireclay, and Keystone – see Table I) were tested (Table II). The Cycletrol clinoptilite was pelletized and tested in the original pelletized form and crushed into a fine powder. The powdered clinoptilite campaign was designated with the letter P in Table II. The illites were tested as received and also after heat treatment (HT) at 750°C for 4 hours to dehydroxylate the clay before reaction in the sealed crucibles. The heat treated illites campaigns were designated with the letters HT in Table II. The as received (AR) illites are designated with the letters AR in Table II.

The presence of 2X sugar in addition to the 53 wt% organics in the EAS simulant on a dry weight basis caused the FBSR products to be overly reduced (Fe²⁺/ΣFe ~1.0 which is all Fe²⁺) and the TOC remaining in the samples to be high 8-14 wt% (Table II) at residence times of 3 hours. Even when no sugar reductant was used, the Fe²⁺/ΣFe remained high at residence times of 3 hours. Residence times of 6 hours without sugar were also overly reduced while residence times of 24 hours without sugar were between a Fe²⁺/ΣFe of 0.5-1.0 depending on the clay type used. Therefore, residence times of 24 hours were chosen for the 1-step and 3-step FBSR simulations in Table III. Since there was a general correlation between the measured TOC and the measured Fe²⁺/ΣFe, and so the TOC was not measured after the first five scoping tests (Table II). The one FPEX sample prepared using 2X sugar and a 24 hour residence time had a Fe²⁺/ΣFe of 0.05.

Bentonite is usually a highly colloidal plastic clay [40] which is actually a mixture of montmorillonite plus either bedellite clay or illite clay. The Fisher bentonite clay was heat treated in the absence of any waste. It formed a mixture of illite and montmorillonite as shown below:



When bentonite was heat treated with EAS waste in the presence of a sugar reductant the measured $Fe^{2+}/\Sigma Fe$ was ~ 1 (corresponding to a residence time of 3 hours): illite formed and the montmorillonite was likely x-ray amorphous Table II. When bentonite was heat treated with EAS waste in the absence of the sugar reductant the measured $Fe^{2+}/\Sigma Fe$ was 0.6-0.8 (corresponding to a residence time of 24-48 hours): the mineral paragonite ($NaAl_3Si_3O_{10}(OH)_2$) formed (Table II). At intermediate residence times the x-ray diffraction analysis indicated that paragonite formed as intermediate phases in the reaction of bentonite and waste to pyrophyllite (dehydrated montmorillonite) and albite as shown below:



Similar to the behavior of the bentonite in the presence of excess reductant, the Sagger XX kaolin based ball clay formed illite at a residence time of 3 hours (EAS-3) but formed pyrophyllite at longer residence times (EAS-11, EAS-19, EAS-26) in agreement with the INL finding of pollucite as a nozzle deposit during FBSR processing. At longer residence times (6-24 hours) in the absence of hydrothermal treatment the Sagger XX clay formed dehydroxylated muscovite (in the absence of excess reductant, depending on residence time (Table II). Both paragonite ($NaAl_3Si_3O_{10}(OH)_2$) and dehydroxylated muscovite ($KAl_3Si_3O_{11}$) are micas.

The IE-95 formed some zeolite like aluminosilicates and the clinopilites formed Na-K-Ca substituted clinoptilites and albite ($NaAlSi_3O_8$). Tests were performed at two FBSR temperatures, $750^\circ C$. and $650^\circ C$ and the same phases were formed at both temperatures. Similar $Fe^{2+}/\Sigma Fe$ ratios were also measured (Table II).

All the illites tested (Table II) and the Sagger XX ball clay campaigns where the clay was pre heat treated formed a single phase, dehydroxylated muscovite ($KAl_3Si_3O_{11}$) which has large XII-fold coordination sites for large cations like Na, K, Cs and Ba. The dehydroxylated muscovite micas, therefore, appear to be promising candidates for the GNEP species and transmutations.

Potassium Nitrate Tests

In some campaigns, KNO_3 was added (Table III). The KNO_3 which denitrates to K_2O was added instead of the full EAS simulant to determine which clays, if any, would encourage the formation of the leucite structure ($KAlSi_2O_6$) which is isostructural with pollucite ($CsAlSi_2O_6$) at FBSR temperatures of $\sim 750^\circ C$. All of the tests were performed with bentonite clay and similar results to the scoping tests were observed:

- at short residence times and excess reductant ($Fe^{2+}/\Sigma Fe \sim 1$) illite formed
- at 24 hour residence times without excess reductant pyrophyllite and albite formed
- at 48 hour residence times without excess reductant paragonite mica formed

One test was performed at $1000^\circ C$ to determine if high temperatures would form leucite but only feldspars and quartz were formed (Table III) indicating that a single leucite/pollucite type phase could not be formed even in the absence of the divalent species present in the GNEP waste streams.

GNEP Waste Stream Tests: Hydrated and Hydrated/Hydrothermal

The SRNL 1-step and 3-step FBSR sequential experiments were performed. A comparison of the data for these tests in Table III indicates that much the same results were obtained with the 1-step and the 3-step experiments. The reactivity of the 3-step experiments appeared to be more complete than the tests with the 1-step process indicating that the 1-step process can be used for scoping tests but the 3-step process should be used for the final determination of the mineral phases produced in these simulated FBSR static tests.

In summary the following conclusions can be made:

- bentonite (montmorillonite) clay and/or Sagger XX kaolin ball clays form multiphase mixtures of hydrated paragonite and major concentrations of excess SiO₂
- illite clays form single phase dehydroxylated muscovites with only minor excess SiO₂
- the muscovites and paragonites were found to tolerate up to 20 wt% GNEP oxides on a dry calcine basis, higher oxide loadings were not tested but likely can be fabricated

The bentonites, which are primarily montmorillonite, are structurally related to the pyrophyllites [41] while the montmorillonites and kaolinities are known to form paragonites [42] when reacted with sodium containing species. The illite clays are structurally related to muscovite [41] which allows greater reactivity when reacted with the large monovalent and divalent species in the GNEP Cs/Sr streams. Since paragonite was likely the aluminosilicate product made by INL from the Cs/Sr simulated waste during FY06 testing and this material performed well in durability testing, either paragonite or Cs-mica (dehydroxylated muscovite) should form acceptable Cs, Rb, Sr, Ba waste forms.

The major difference between the paragonite Na-rich mica and the K-rich muscovite mica is that the XII-fold coordinated sites that hold the Na and K cations are different. The XII-fold site is formed by an six-membered oxygen ring of the layer above and below it. The smaller the cation in between the two layers the more the repulsive charges of each layer force the layers apart. Thus the XII-fold site in paragonite is smaller and more irregular than that in the muscovite micas [41]. This may make paragonite structure less tolerant of Cs-137 decay to Ba-137 and Sr-90 transmutations to Y-90 and Zr-90. In the muscovites, ¼ of the tetrahedral (IV-fold coordination) sites are filled by Al³⁺ while the rest of the Al³⁺ is octahedral (VI-fold coordination). For the K-rich muscovites the following is known [41, 43]:

- Na, Rb, Cs, Ca, Ba, La, Tl, Sr can substitute in the XII-fold sites
- Mg, Fe²⁺, Fe³⁺, Mn, Li, Cr, Ti and V can substitute for VI-fold coordinated Al³⁺

The following dehydroxylated micas have been synthesized phase pure [43]: LiAl₃Si₃O₁₁, NaAl₃Si₃O₁₁, KAl₃Si₃O₁₁, RbAl₃Si₃O₁₁, CsAl₃Si₃O₁₁, TlAl₃Si₃O₁₁, Ca_{0.5}□_{0.5}Al₃Si₃O₁₁, Sr_{0.5}□_{0.5}Al₃Si₃O₁₁, Ba_{0.5}□_{0.5}Al₃Si₃O₁₁, La_{0.33}□_{0.66}Al₃Si₃O₁₁. In the Cs-mica up to 30 wt% Cs₂O can be accommodated, in the Rb-mica up to 22 wt% Rb₂O can be accommodated, and in the Ba-mica up to 19 wt% BaO can be accommodated.

GNEP Waste Stream Tests: Multiphase Pollucite-Celsian Formation at 1000°C

Pollucite was made from a bentonite-Fe₂O₃ mixture with CsNO₃ and Sr(NO₃)₂ using a PNNL formulation that only accommodated ~15-16 wt% Cs-Sr oxides. Testing was carried out at 1000°C instead of PNNL's recommended 1200°C due to concerns about Cs volatility and in order to be more prototypic of Argonne National Laboratory's (ANL) sintered bentonite process.

Table II REDOX, Residence Time, Clay Type, and Clay Heat Treatment Test Matrix

Test ID	Temp (°C)	Time (Hrs.)	Sugar None	Sugar 2X	Clay or Zeolite	Major Phases Identified by X-Ray Diffraction	Minor Phases Identified by X-Ray Diffraction	TOC (wt%)	Fe ⁺² ΣFe
EAS-1A	750	3	X		Bentonite AR	Paragonite	SiO ₂ (Quartz)	<0.07	0.56
EAS-1B	750	3		X	Bentonite AR	Quartz (SiO ₂) + Illite	NONE	8.14	0.97
EAS-2A	750	3	X		Bentonite AR	Paragonite	SiO ₂ (Quartz)	<0.07	0.81
EAS-2B	750	3		X	Bentonite AR	Quartz (SiO ₂) + Illite	NONE	13.4	1.0
EAS-3	750	3		X	Sagger XX Fine AR	Quartz (SiO ₂) + Illite	TiO ₂	14.0	1.0
EAS-5A	750	3		X	Cycletrol Clinoptilite	(Na,K,Ca)Al ₆ Si ₃ O ₇₂ •18H ₂ O (Na-clinoptilite) + SiO ₂ (Quartz)	MgSi ₄ O ₁₀ (OH) ₂ (Talc) + Albite	NM	0.93-1.0
EAS-5P	650	3		X	Cycletrol Clinoptilite	(Na,K,Ca)Al ₆ Si ₃ O ₇₂ •18H ₂ O (Na-clinoptilite) + SiO ₂ (Quartz)	Albite + Magnetite	NM	1.0
EAS-9A	750	24	X		Bentonite AR	Pyrophyllite + Albite + SiO ₂ (Cristobalite)	SiO ₂ (Quartz)	NM	0.47
EAS-9B	750	48	X		Bentonite AR	Paragonite + SiO ₂ (Cristobalite)	SiO ₂ (Quartz)	NM	NM
EAS-11	750	24	X		Sagger XX Fine AR	Pyrophyllite	SiO ₂ (Quartz) + TiO ₂	NM	0.80
EAS-12	750	24	X		Snow White Clinoptilite	Albite + Clinoptilite + SiO ₂ (Quartz)	Pyrophyllite + Fe ^o	NM	1.0
EAS-13A	750	6	X		Bentonite AR	Pyrophyllite + Albite + SiO ₂ (Cristobalite)	SiO ₂ (Quartz)	NM	0.90-0.92
EAS-13B	750	48	X		Bentonite AR	Pyrophyllite + SiO ₂ (Cristobalite)	SiO ₂ (Quartz)	NM	1.0
EAS-15	750	6	X		Illite Redart AR	(Cs,K)-mica + SiO ₂ (Quartz)	NONE	NM	0.60-1.0
EAS-18	750	6	X		Illite Redart HT	(Cs,K)-mica + SiO ₂ (Quartz)	NONE	NM	1.0
EAS-19	750	6	X		Sagger XX Fine AR	Pyrophyllite + SiO ₂ (Quartz)	TiO ₂	NM	0.80-0.88
EAS-21	750	6	X		Illite Fireclay AR	(Cs,K)-mica + SiO ₂ (Quartz)	TiO ₂	NM	0.95-1.0
EAS-23	750	6	X		Illite Todd Light AR	(Cs,K)-mica + SiO ₂ (Quartz)	NONE	NM	0.9-1.0
EAS-25	750	6	X		Illite Todd Light HT	(Cs,K)-mica + SiO ₂ (Quartz)	TiO ₂	NM	0.27
EAS-26	750	6	X		Sagger XX Fine HT	Pyrophyllite + SiO ₂ (Quartz)	TiO ₂	NM	0.85
EAS-27	750	6	X		Illite Fireclay AR + HT	(Cs,K)-mica + SiO ₂ (Quartz)	TiO ₂	NM	0.67
EAS-29	750	6	X		Illite Keystone HT	(Cs,K)-mica + SiO ₂ (Quartz)		NM	0.63
EAS-36	750	6	X		IE-95	K _{2,04} Na _{0,06} Al ₂ Si _{7,8} O _{20,7}	Na ₂ Al ₂ Si ₆ •H ₂ O	NM	1.0

(Cs,K)-mica = KAl₃Si₃O₁₁ = Dehydroxylated muscovite

Pyrophyllite = Al₂Si₄(OH)₁₀ (OH)

Paragonite = NaAl₂Si_{2,98}Al_{1,02}O₁₀(OH)₂

Illite = K_{0,7}Al₂(Si,Al)₄O₁₀(OH)₂

Albite = NaAlSi₃O₈

Table III. KNO₃ Tests, Anhydrous Tests, and Mixed Anhydrous/Hydrous Tests

Test ID	Temp (°C)	Time (Hrs.)	WL Calcine Oxide (Cs,Rb, Sr,Ba) Wt%	Sugar None	Sugar 2X	Clays As Received	K ₂ O (Wt%)	Major Phases Identified by X-Ray Diffraction	Minor Phases Identified by X-Ray Diffraction	TOC (wt%)	Fe ⁺² ΣFe
TRIALS WITH KNO₃											
EAS-1C	750	3	N/A		X	Bentonite	10	SiO ₂ (Quartz) + Illite	NONE	8.87	0.97
EAS-2C	750	3	N/A		X	Bentonite	10	SiO ₂ (Quartz) + Illite	NONE	17.8	1.0
EAS-10A	750	24	N/A	X		Bentonite	10	Pyrophyllite + Albite + SiO ₂ (Cristobalite)	SiO ₂ (Quartz)	NM	0.05
EAS-10B	750	48	N/A	X		Bentonite	10	Pyrophyllite + SiO ₂ (Quartz)	Cristobalite	NM	NM
EAS-10C	1000	6	N/A	X		Bentonite	10	SiO ₂ (Cristobalite + Quartz)	Anorthite (Ca,Na)(Al,Si) ₂ Si ₂ O ₈ + Fe ₂ O ₃	NM	NM
HYDRATED TRIALS (1 STEP)											
EAS 2-1	750	24	5	X		Bentonite	N/A	15 Å Montmorillonite + Paragonite + SiO ₂ (Cristobalite)	SiO ₂ (Quartz)	NM	NM
EAS 2-2	750	24	10	X		Bentonite	N/A	15 Å Montmorillonite + Paragonite + SiO ₂ (Cristobalite)	SiO ₂ (Quartz)	NM	NM
EAS 2-3	750	24	15	X		Bentonite	N/A	Paragonite + SiO ₂ (Cristobalite + Quartz)	15 Å Montmorillonite	NM	NM
EAS 2-4	750	24	20	X		Bentonite	N/A	Paragonite + SiO ₂ (Quartz)	NONE	NM	NM
EAS 2-5	750	24	10	X		Sagger XX	N/A	Paragonite + SiO ₂ (Quartz)	TiO ₂	NM	NM
EAS 2-6	750	24	20	X		Sagger XX	N/A	Paragonite + SiO ₂ (Quartz)	TiO ₂	NM	NM
EAS 2-7	750	24	10	X		Illite Redart	N/A	(Cs,K)-mica + Albite + SiO ₂ (Quartz)	Al ₂ O ₃	NM	NM
EAS 2-8	750	24	20	X		Illite Redart	N/A	(Cs,K)-mica + Albite	SiO ₂ (Quartz)	NM	NM
HYDRATED/HYDROTHERMAL/HYDRATED TRIALS (3 STEP)											
EAS 2-4 (3)	750	24	20	X		Bentonite	N/A	Paragonite + SiO ₂ (Cristobalite + Quartz)	NONE	NM	NM
EAS 2-6 (3)	750	24	20	X		Sagger XX	N/A	Paragonite + SiO ₂ (Quartz)	Al ₂ O ₃	NM	NM
EAS 2-8 (3)	750	24	20	X		Redart	N/A	(Cs,K)-mica	SiO ₂ (Quartz)	NM	NM

15 Å Montmorillonite = (Na₃(Al,Mg)₂Si₄O₁₀(OH)₂•4H₂O

(Cs,K)-mica = KAl₃Si₃O₁₁ = Dehydroxylated muscovite

Pyrophyllite = Al₂Si₄(OH)₁₀ (OH)

Paragonite = NaAl₂Si_{2.98}Al_{1.02}O₁₀(OH)₂

Illite = K_{0.7}Al₂(Si,Al)₄O₁₀(OH)₂

Albite = NaAlSi₃O₈

The ANL process produces pollucite and Sr-feldspars, the PNNL process produces pollucite and celsian (a Ba feldspar, $\text{BaAl}_2\text{Si}_2\text{O}_8$). In SRNL's trials pollucite, Sr feldspar ($\text{SrAl}_2\text{Si}_2\text{O}_8$), and Fe_2O_3 were found to form at 1000°C but Fe, Cs, and Sr all appeared to be present in different phases which is not conducive for accommodating cation transmutations.

CONCLUSIONS

A single phase mineralized (Cs,K)-mica phase can be made by co-reacting illite clay and a GNEP simulated waste containing Cs, Ba, Sr, and Rb. The (Cs,K)-mica accommodates up to 20% wt% of the GNEP waste species on an oxide basis (potentially higher concentrations were not tested in this study). The (Cs,K)-mica has the potential to accommodate the Cs-137 transmutation to Ba-137 and the Sr-90 transmutation to Y-90 because $\text{RbAl}_3\text{Si}_3\text{O}_{11}$, $\text{CsAl}_3\text{Si}_3\text{O}_{11}$, $\text{Ba}_{0.5}\square_{0.5}\text{Al}_3\text{Si}_3\text{O}_{11}$ and $\text{La}_{0.33}\square_{0.66}\text{Al}_3\text{Si}_3\text{O}_{11}$ micas with identical structures (and their Fe^{3+} analogs) are known to form. These micas are dehydroxylated and contain no H_2O or OH^- species that could generate radiolytic hydrogen. The (Cs,K)-mica can be made by the FBSR process which simultaneously destroys the organics and nitrates, does not produce secondary aqueous wastes, and is a CAA compliant technology. The FBSR process operates at $650\text{-}750^\circ\text{C}$.

ACKNOWLEDGEMENTS

This work was funded through the Separations Campaign under the Technical Integration Office of the Global Nuclear Energy Partnership, Office of Nuclear Energy, U.S. DOE and in connection with work done under Contract No. DE-AC09-96SR18500 with the U.S. Department of Energy (DOE).

REFERENCES

- 1 C.M. JANTZEN and F.P. GLASSER, "Crystallochemical Stabilization of Radwaste Elements in Portland Cement Clinker," *Proceed. Intl. Symp. Ceramics in Nucl. Waste Mgt; CONF-790420*, 342-348 (1979).
- 2 C.M. JANTZEN and F.P. GLASSER, "Stabilization of Nuclear Waste Constituents in Portland Cement," *Am. Ceram. Soc. Bull.*, 58[4], 459-66 (1979).
- 3 R.D. SHANNON and C.T. PREWITT, "Effective Ionic Radii in Oxides and Fluorides," *Acta. Cryst.*, B25, 925-946 (1969).
- 4 R.D. SHANNON and C.T. PREWITT, "Revised Values of Effective Ionic Radii," *Acta. Cryst.*, B26, 1046-1048 (1970).
- 5 J. FELSCHE, "Rare Earth Silicates with the Apatite Structure," *J. Solid State Chem*, 5[2], 266-275 (1972).
- 6 G.J. McCARTHY and M.T. DAVIDSON, "Ceramic Nuclear Waste Forms" *Am. Ceram. Soc. Bull.*, 54[9], 782-86 (1975).
- 7 F.M. LEA, "The Chemistry of Cement and Concrete," Edward Arnold Publishers Ltd., 727pp (1970).
- 8 C.M. JANTZEN and F.P. GLASSER, and E.E. LACHOWSKI, "Radioactive Waste-Portland Cement Systems: I. Radionuclide Distribution," *J. Am. Ceram. Soc.*, 67 [10], 668-673 (1984).
- 9 C.M. JANTZEN and F.P. GLASSER, and E.E. LACHOWSKI, "Radioactive Waste-Portland Cement Systems: II. Leaching Characteristics," *J. Am. Ceram. Soc.*, 67 [10], 674-678 (1984).
- 10 A.E. RINGWOOD and S.E. KESSON, "Immobilization of High-Level Wastes in Synroc Titanate Ceramic," *Proceed. Intl. Symp. Ceramics in Nucl. Waste Mgt; CONF-790420*, 174-178 (1979).
- 11 P.E.D. MORGAN, D.R. CLARKE, C.M. JANTZEN, and A.B. HARKER, "High Alumina Tailored Nuclear Waste Ceramics," *J. Am. Ceram. Soc.*, 64[5], 249-258 (1981).
- 12 C.M. JANTZEN, D.R. CLARKE, P.E.D. MORGAN, and A.B. HARKER, "Leaching of Polyphase Nuclear Waste Ceramics: Microstructural and Phase Characterization," *J. Am. Ceram. Soc.*, 65[6], 292-300 (1982).
- 13 J.A. COOPER, D.R. COUSENS, R.A. LEWIS, S. MYHRA, R.L. SEGALL, R.St.C. SMART, P.S. TURNER, and T.J. WHITE, "Microstructural Characterization of Synroc C and E by Electron Microscopy," *J. Am. Ceram. Soc* 68 [2] 64-70 (1985).
- 14 V. AUBIN, D. CAURANT, D. GOURIER, N. BAFFIER, T. ADVOCAT, F. BART, G. LETURCQ, and J.M. COSTANTINI, "Synthesis, Characterization and Study of the Radiation Effects on Hollandite Ceramics Developed for Cesium Immobilization," *Mat. Res. Soc. Symp. Proc. V. 807*, 315-320 (2004).

- 15 K.P. HART, E.R. VANCE, R.A. DAY, B.D. BEGG, and P.J. ANGEL "Immobilization of Separated Tc and Cs/Sr in SYNROC," *Mat. Res. Soc. Symp. Proc.* V. 412, 281-287 (1996).
- 16 W.D. TOWNES, J.H. FANG, and A.J. PERROTTA, "The Crystal Structure and Refinement of Ferromagnetic Barium Ferrite, BaFe₁₂O₁₉," *Z. Kristallogr.* 125, 437-49 (1967).
- 17 D.M. STRACHAN and W.W. SCHULZ, "Characterization of Pollucite as a Material for Long-Term Storage of Cesium-137," *Am. Ceram. Soc. Bull.*, V58 [9], 865-871 (1979).
- 18 W.A. DEER, R.A. HOWIE, W.S. WISE, and J. ZUSSMAN, "Rock-Forming Minerals Framework Silicates: Silica Minerals, Feldspathoids and the Zeolites," Vol. 4B, *Geol. Soc. of London, London*, 982pp (2004).
- 19 C.M. JANTZEN, "Engineering Study of the Hanford Low Activity Waste (LAW) Steam Reforming Process," U.S. DOE Report WSRC-TR-2002-00317, Westinghouse Savannah River Co., Aiken, SC (July, 2002).
- 20 C.M. JANTZEN, "FBSR of Organic and Nitrate Containing Salt Supernate," *Ceram. Trans.* 168, 68-79 (2005).
- 21 C.M. JANTZEN, "Disposition of Tank 48H Organics by Fluidized Bed Steam Reforming (FBSR)," U.S. DOE Report WSRC-TR-2003-00352 (September 18, 2003).
- 22 J.B. MASON, J. McKIBBEN, K. RYAN and D. SCHMOKER, "Steam Reforming Technology for Denitration and Immobilization of DOE Tank Wastes," *Waste Management 03* (2003).
- 23 N.R. SOLEBERG, D.W. MARSHALL, S.O. BATES, and D.D. TAYLOR, "Phase 2 THOR Steam Reforming Tests for Sodium Bearing Waste Treatment," U.S. DOE Report INEEL/EXT-04-01493, Rev. 1 (2004).
- 25 C.M. JANTZEN, "Characterization and Performance of Fluidized Bed Steam Reforming (FBSR) Product as a Final Waste Form," *Ceramic Transactions* 155, 319-329 (2004).
- 25 J.M. PAREIZS, C.M. JANTZEN, and T.H. LORIER, "Durability Testing of Fluidized Bed Steam Reformer (FBSR) Waste Forms for High Sodium Wastes at Hanford and Idaho," U.S. DOE Report WSRC-TR-2005-00102 (2005).
- 26 C.M. JANTZEN, J.M. PAREIZS, T.H. LORIER, and J.C. MARRA, "Durability Testing of Fluidized Bed Steam Reforming (FBSR) Products," *Ceramic Transactions*, 176, 121-137 (2005).
- 27 C.M. JANTZEN, T.H. LORIER, J.C. MARRA, and J.P. PAREIZS, "Durability Testing of Fluidized Bed Steam Reforming (FBSR) Waste Forms," *Waste Management '06*, Paper #6373 (2006).
- 28 C.L. CRAWFORD and C.M. JANTZEN, "Durability Testing of Fluidized Bed Steam Reformer (FBSR) Waste Forms for Sodium Bearing Waste (SBW) at INL" WSRC-STI-2007-00319 (August 2007).
- 29 B.P. McGRAIL, H.T. SCHAEF, P.F. MARTIN, D.H. BACON, E.A. RODRIQUEZ, D.E. McCREADY, A.N. PRIMAK, and R.D. ORR, "Initial Evaluation of Steam-Reformed Low Activity Waste for Direct Land Disposal," U.S. DOE Report PNWD-3288 (2003).
- 30 T.H. LORIER, J.M. PAREIZS, and C.M. JANTZEN, "Single Pass Flow Through (SPFT) Testing of Fluidized Bed Steam Reforming (FBSR) Waste Forms," U.S. DOE Report, WSRC-TR-2005-00124 (2005).
- 31 C.M. JANTZEN, T.H. LORIER, J.M. PAREIZS, and J.C. MARRA, "FBSR Mineral Waste Forms: Characterization and Durability Testing," *Sci. Basis Nucl. Waste Mgt.* XXX, 379-386 (2007).
- 32 B.P. McGRAIL, "Laboratory Testing of Bulk Vitriified and Steam-Reformed Low-Activity Forms to Support a Preliminary Assessment for an Integrated Disposal Facility," U.S. DOE Report PNNL-14414 (2003).
- 33 E. PUURA and I. NERETNIEKS, "Atmospheric Oxidation of the Pyritic Waste Rock in Maardu, Estonia, 2: An Assessment of Aluminosilicate Buffering Potential," *Environ Geol.* 39 [6], 560-566 (2000).
- 34 C.M. JANTZEN, "Fluidized Bed Steam Reformer (FBSR) Product: Monolith Formation and Characterization," U.S. DOE Report WSRC-STI-2006-00033 (June 2006).
- 35 C.M. JANTZEN, "Fluidized Bed Steam Reformer (FBSR) Monolith Formation," WM07, Paper #7075 (2007).
- 36 T.G. HINTON, D.I. Kaplan, A.S. KNOX, D.P. COUGHLIN, R.V. NASCIMENTO, S.I. WATSON, D.E. FLETCHER, and B.J. KOO, "Use of Illite Clay for In Situ Remediation of 137Cs-Contaminated Water Bodies: Field Demonstration of Reduced Biological Uptake," *Environ. Sci. Technol.*, 40, 4500-4505 (2006).
- 37 C.M. JANTZEN, "Disposition of Tank 48H Organics by Fluidized Bed Steam Reforming (FBSR)," U.S. DOE Report WSRC-TR-2003-00352 (September 18, 2003).
- 38 N. SOELBERG, D. MARSHALL, S.O. BATES and D. SIEMER, "SRS Tank 48 Steam Reforming Proof-of-Concept Test Results," INEEL/EXT-03-01118 (2004).
- 39 E.W. BAUMANN, "Colorimetric Determination of Iron(II) and Iron(III) in Glass," *Analyst*, 117, 913-916 (1992).
- 40 R.E. GRIMM, "Clay Mineralogy," McGraw Hill Book Co., New York, 384pp (1953).
- 41 W.A. DEER, R.A. HOWIE, J. ZUSSMAN, "Rock Forming Minerals," V. 3, Longmans, London, 270p (1965).
- 42 W.A. DEER, R.A. HOWIE, J. ZUSSMAN, "Rock Forming Minerals," V. 3A, *Geol. Soc.*, London, 758p (2003).
- 43 H. KEPPLER, "Ion Exchange Reactions Between Dehydroxylated Micas and Salt Melts and the Crystal Chemistry of the Interlayer Cation in Micas," *Am. Min.* V. 75, 529-538 (1990).